nature cities

Article

https://doi.org/10.1038/s44284-025-00290-2

Standardized heat islands and persistence drive modeled urban heat events

Received: 24 September 2024

Accepted: 3 July 2025

Published online: 01 August 2025

Check for updates

Weilin Liao[1,2], Linying Wang[3,4], Xiaoping Liu[1,2] ✉, Duo Chan[5] ✉ & Dan Li[4,6] ✉

Urban environments are usually hotter than their rural surroundings, a phenomenon known as the urban heat island (UHI) effect. The mean UHI effect implies that urban environments would experience more heat events if the same temperature threshold is used to identify heat events in both urban and rural environments. However, the role of higher-order temperature statistics, such as temperature variance and persistence, in determining urban–rural differences of heat event occurrence remains elusive. Here, using numerical simulations from two global models, we demonstrate that up to 94% of urban–rural differences in hot day occurrence are driven by the mean UHI effects normalized by temperature variance, that is, the standardized mean UHI effects. For multi-day heat events, temperature persistence further plays an important role. These findings reveal how the temperature mean, variance and persistence interact to determine the urban–rural difference in heat event occurrence. Cities with more pronounced standardized mean UHI effects and enhanced temperature persistence should place greater emphasis on mitigating the adverse impacts caused by extreme heat.

Extreme heat has multifaceted effects that negatively impact human society (for example, health, air quality, energy consumption and water use) and is widely recognized as the dominant weather-related cause of mortality[1–3]. The casualties caused by extreme heat far exceed those caused by other extreme weather events such as droughts, floods and storms. Between 2000 and 2019, approximately 489,000 people died each year globally due to extreme heat. Even worse, climate models predict that the frequency, duration and intensity of heat extremes will probably increase in the coming decades[1,4,5].

Currently, there are no universal definitions for extreme heat events. For hot days, defined as single days with the temperature exceeding a specific threshold, changes in the probability of their occurrence can be attributed to two primary factors: changes in mean temperature and changes in temperature variability[6–8]. This framework has been extensively used to examine how hot day occurrence is affected by climate change. Studies have shown that changes in hot day occurrence are principally due to an increase in mean temperatures[9], and this finding is robust under various future climate scenarios[10]. However, extreme heat events can also be (and usually are) defined as a period of consecutive hot days. For such multi-day heat events, temperature persistence needs to be further considered[10]. Recent works reported differences in temperature persistence between urban and rural environments[11] and widespread changes in temperature persistence under climate change[6].

Urbanization has caused a distinctive phenomenon known as the urban heat island (UHI) effect, which renders urban areas, on average, hotter than their rural counterparts[12,13]. This mean UHI effect will increase the hot day occurrence in urban environments than in rural environments if one uses the same temperature threshold to define hot days for both urban and rural environments[14–17], and this applies

[1]Guangdong Key Laboratory for Urbanization and Geo-simulation, School of Geography and Planning, Sun Yat-sen University, Guangzhou, China. [2]Southern Marine Science and Engineering Guangdong Laboratory (Zhuhai), Zhuhai, China. [3]National Key Laboratory of Earth System Numerical Modeling and Application, Institute of Atmospheric Physics, Chinese Academy of Sciences, Beijing, China. [4]Department of Earth and Environment, Boston University, Boston, MA, USA. [5]School of Ocean and Earth Science, University of Southampton, Southampton, UK. [6]Department of Mechanical Engineering, Boston University, Boston, MA, USA. ✉e-mail: liuxp3@mail.sysu.edu.cn; Duo.Chan@soton.ac.uk; lidan@bu.edu

https://doi.org/10.1038/s44284-025-00290-2

to multi-day heat events, too. However, it remains unclear how urban–rural differences in higher-order temperature statistics (for example, variance and persistence), if they exist, contribute to urban–rural differences in hot day and multi-day heat event occurrences. Hence, the critical research question that motivates this work pertains to how differences in mean and higher-order temperature statistics interact and increase the occurrence of heat events in urban compared with rural environments. Here we address this question using numerical simulations from two global models, that is, the Geophysical Fluid Dynamics Laboratory (GFDL) land model LM4, coupled with a newly developed and evaluated Urban Canopy Model (UCM) and the Community Land Model (CLM), which is the land component of the Community Earth System Model (CESM; Methods). A multivariate Gaussian framework is then used to understand and predict the urban–rural difference in the probability of heat event occurrence simulated by global models. Here we will only focus on the summer season.

Results

Standardized mean UHI effects explain urban–rural differences in hot day occurrence

In this section, we focus on urban–rural differences in the occurrence of hot days, which are identified using the same temperature threshold (that is, the 90th percentile of rural temperatures) for both urban and rural environments. The probability of hot day occurrence, defined as the frequency of daily temperatures higher than the threshold, is denoted as HDP_u and HDP_r for urban and rural environments, respectively. Figure 1a shows a schematic for this urban–rural difference in the probability of hot day occurrence, for which both temperature mean and variance could differ and contribute, similar to the difference between future and present climates under global warming scenarios.

Figure 2a,b shows the spatial distribution of simulated urban–rural differences in the probability of hot day occurrence ($\delta HDP = HDP_u - HDP_r$) in the GFDL and CLM models, respectively. In general, δHDP ranges from −0.05 to 0.4 in the GFDL model and from 0 to 0.7 in the CLM model. Despite this difference in magnitude, both models exhibit high δHDP values in the eastern United States, Europe and Asia. This spatial pattern resembles the mean urban–rural temperature difference (that is, mean UHI) pattern simulated by both models (Supplementary Fig. 1). The correlation coefficients between the mean UHI and δHDP is 0.63 for the GFDL and 0.53 for the CLM model, suggesting an important role of mean UHI in controlling the urban–rural difference in hot day occurrence.

To further elaborate the role of mean UHI, a standardized univariate Gaussian theory is proposed, which uses the cumulative density function (CDF) of normal distribution with a standard error of unity to predict the occurrence of hot days (Methods). Two assumptions are crucial for the standardized Gaussian framework. First, daily temperatures are assumed to follow Gaussian distributions in both urban and rural areas. Such an assumption is motivated by existing studies[9,10] and allows for an analytical expression for hot day occurrence using only the mean and variance. Some regions may exhibit positive skewness[18] and do not strictly follow a Gaussian distribution. However, less than 11.9% of the analyzed grid cells (defined as grid cells with urban fraction exceeding 0.1%) in the GFDL model and 11.4% in the CLM model show significant urban–rural differences in skewness at the 95% confidence level based on the Fisher–Pearson test. Hence, as our results below indicate, this standardized Gaussian framework still reproduces the simulated urban–rural differences in hot day occurrence reasonably well.

Second, the variances of urban and rural temperatures are assumed to be similar, that is, $\sigma_u \approx \sigma_r$, where σ_u and σ_r are the standard deviations for urban and rural temperatures, respectively. This assumption is inferred from a direct validation by performing Levene's test on a grid level, which suggests that σ_u and σ_r show no statistically significant difference at the 95% confidence level over 72.2% of the analyzed grid cells in the GFDL model and 50.3% in the CLM model (Supplementary Fig. 2).

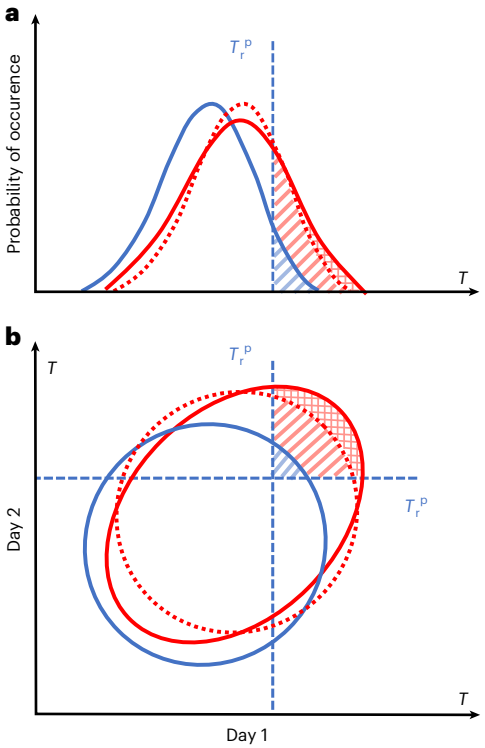

Fig. 1 | Schematic of urban–rural differences in the probability of hot day and multi-day heat event occurrences. a,**b**, Hot days (**a**) and heat events (**b**) of at least two consecutive days. The shaded areas represent the probability of heat event occurrence in urban (in both red- and blue-shaded areas; HDP_u) and rural (in blue-shaded area; HDP_r) environments defined using the rural temperature threshold (T_r^P, which is set to be the 90th or 95th percentile of rural climatology). Meanwhile, the shaded area with red diagonal lines represents an increase in the probability of heat event occurrence in the urban environment due to urban–rural difference in the mean temperature. The shaded area with red cross-hatch lines indicates the increase in probability of heat event occurrence in the urban environment due to the urban–rural difference in higher-order temperature statistics, that is, temperature variance and persistence.

On average, the global mean of the absolute (relative) urban–rural difference in temperature standard deviation is only 0.016 °C (1.4%) in the GFDL model and 0.063 °C (3.7%) in the CLM model.

Under these two assumptions, the urban–rural difference in the probability of hot day occurrence (δHDP) is solely a function of the standardized mean UHI (δZ):

$$\delta HDP = HDP_u - HDP_r = \phi(\Gamma) - \phi(\Gamma - \delta Z), \quad (1)$$

where ϕ is the CDF of a zero-centered Gaussian distribution with standard error of unity, $\delta Z = UHI/\sigma_r$ is the mean UHI normalized by the standard deviation of rural temperature (which is equivalent to UHI/σ_u in our framework) and Γ is the threshold for identifying hot days. A more detailed closed-form analytical expression is provided in Methods.

Figure 2e,f shows the relation between δHDP and δZ for hot days. The model simulations align closely with the standardized Gaussian framework (equation (1)), with the root mean square error (RMSE) of 0.017 in the GFDL model and 0.021 in the CLM model. Compared with the δHDP values, which are 0.031 ± 0.063 (mean ± one standard deviation) in the GFDL model and 0.101 ± 0.093 in the CLM model, the RMSE values are small. Overall, the theoretical curve can explain 94.3% (estimated by the coefficient of determination (R^2)) of the diagnosed δHDP in the GFDL model and 95.6% in the CLM model. These findings demonstrate that δHDP for hot days can be largely predicted by the standardized mean UHI. Here we highlight that the importance of δZ

https://doi.org/10.1038/s44284-025-00290-2

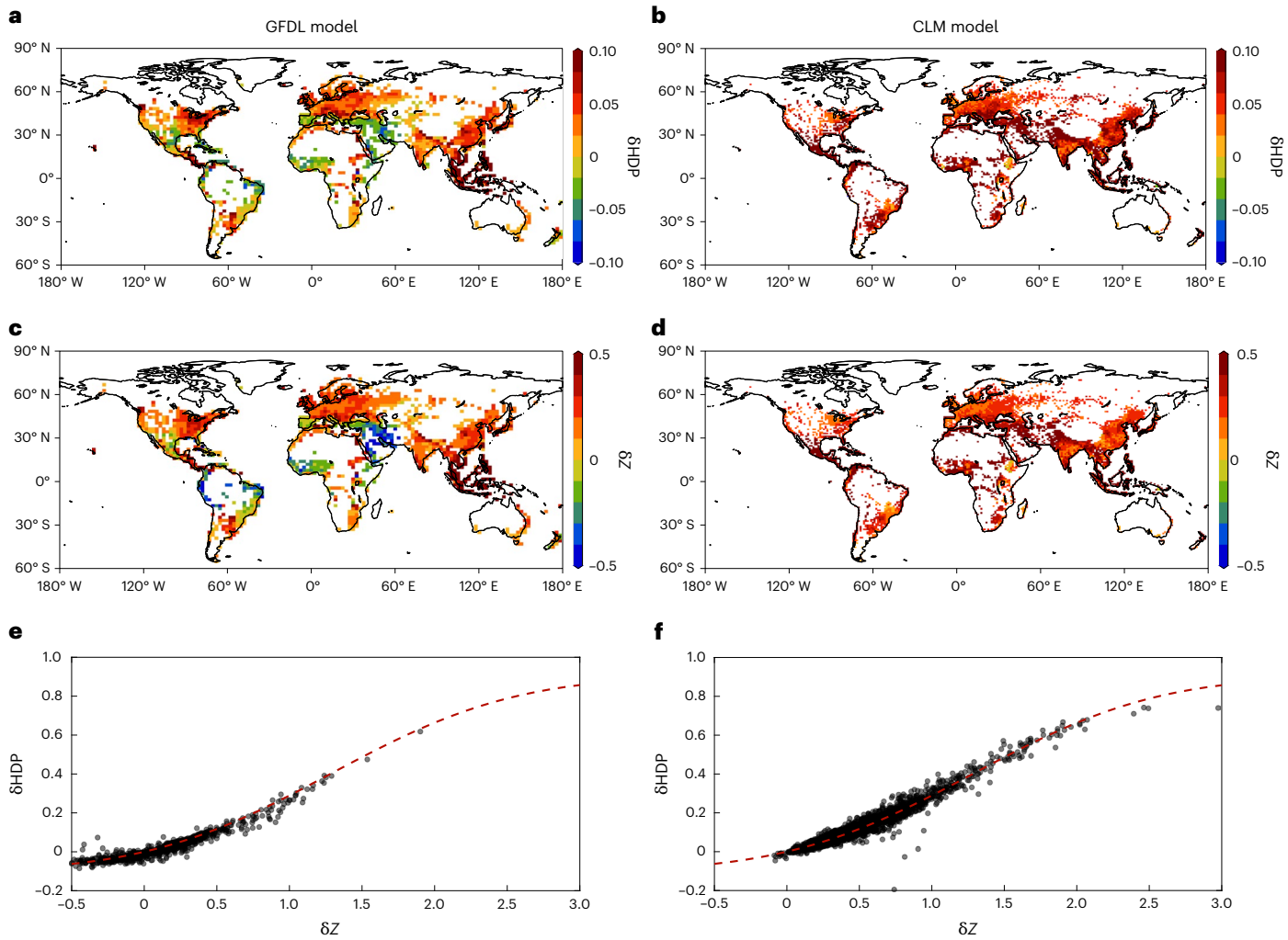

Fig. 2 | Relation between δHDP and δ*Z* for hot days. a,**b**, Spatial patterns of δHDP. **c**,**d**, Spatial spatterns of δ*Z*. **e**,**f**, Comparison of the standardized Gaussian framework (red dashed lines calculated using equation (1)) with the global model simulation data. Left column: results from the GFDL model (**a**, **c** and **e**); right column: from the CLM model (**b**, **d** and **f**).

in predicting δHDP is consistent between the GFDL and CLM models, even though the two models produce fairly different mean UHI effects. Moreover, here we use the 90th percentile threshold for defining hot days, but the results are qualitatively similar when using another threshold (Supplementary Fig. 3). The standardized Gaussian framework can explain 86.5% and 93.3% for the 95th percentile threshold in the GFDL and CLM models, respectively. The degradation of performance as the percentile threshold increases is partly related to the reduced sample size (that is, the number of hot days is reduced when using the 95th percentile threshold).

Importance of temperature persistence for multi-day heat events

When heat events are defined as periods with temperatures warmer than the threshold for at least two or more consecutive days, temperature persistence, which can be quantified by temporal autocorrelation (AC), needs to be further considered[10]. As the AC increases, it becomes easier to trigger longer-duration heat events (Fig. 1b). Therefore, urban–rural differences in the probability of multi-day heat event occurrence (that is, urban–rural differences in the yearly sum of days participating in multi-day heat events) can be influenced not only by the standardized mean UHI but also by the temperature persistence.

As a starting point, we assume that both urban and rural temperatures are independent across days, and thus, the urban–rural difference in the probability of *N*-day heat event occurrence can be expressed by an *N*-dimensional Gaussian distribution:

$$\delta\mathrm{HDP} = \phi_N(\Gamma) - \phi_N(\Gamma - \delta Z), \tag{2}$$

where ϕ_N is the CDF of an *N*-dimensional Gaussian distribution centered on zero. This model does not capture the δHDP value simulated by climate models well, especially when δ*Z* is greater than 0.5 (Fig. 3). The overall RMSE is 0.029 in the GFDL model and 0.061 in the CLM model (Fig. 4a,b), and equation (2) explains only 82.6% of the diagnosed δHDP in the GFDL model and 86.8% in the CLM model when heat events are defined as periods lasting at least 2 consecutive days (hereafter referred to as 2-day heat events; Fig. 3a,b). Compared with the results for single hot days, the explanatory power of equation (2) decreases by 11.7% in the GFDL model and 8.8% in the CLM model. Meanwhile, when heat events are defined as periods lasting at least 3 consecutive days (hereafter referred to as 3-day heat events), the overall RMSE even increases to 0.038 in the GFDL model and 0.075 in the CLM model (Fig. 4c,d), and equation (2) explains only 58.0% of the diagnosed δHDP in the GFDL model and 71.4% in the CLM model (Fig. 3c,d). Compared with the results for single hot days, the explanatory power of equation (2)

https://doi.org/10.1038/s44284-025-00290-2

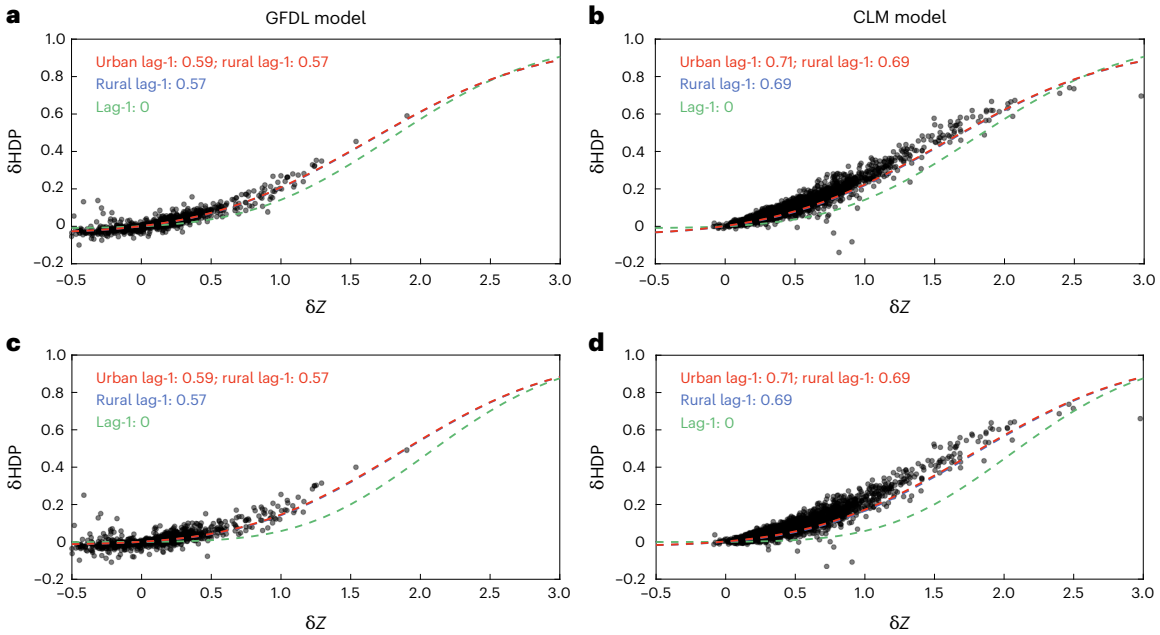

Fig. 3 | Impact of temperature persistence on δHDP for multi-day heat events with different lag-1 AC assumptions. a,**b**, Comparison of climate model simulation data with different statistical models (equations (2)–(4)) for two-day heat events. **c**,**d**, Results for three-day heat events. Green dashed lines assume that urban and rural daily mean temperatures are independent across days (equation (2)). Blue dashed lines assume that both urban and rural temperature series adopt the same lag-1 AC value calculated by the global average lag-1 AC of rural temperature series (equation (3)). The red dashed lines assume that urban temperature series have a lag-1 AC value matching the global urban average, and rural temperatures have a lag-1 AC equal to the global rural average (equation (4)). Given the similarity between the global urban and rural lag-1 AC averages, the differences between the blue and red lines are small. Left column: results from the GFDL model (**a** and **c**); right column: from the CLM model (**b** and **d**).

decreases by 36.3% in the GFDL model and 24.2% in the CLM model. Overall, these results imply that δHDP for multi-day heat events may be influenced not only by the standardized mean UHI but also by the temperature persistence.

Accordingly, we extend the framework to an N-dimensional multivariate Gaussian distribution. Assuming that urban and rural temperatures share the same lag-1 AC calculated from the rural temperature within each grid, the urban–rural difference in the probability of N-day heat event occurrence can be expressed as

$$\delta\mathrm{HDP} = \phi_N(\Gamma, \alpha_\mathrm{r}) - \phi_N(\Gamma - \delta Z, \alpha_\mathrm{r}), \quad (3)$$

where the multivariate Gaussian distribution has a covariance matrix Σ defined as $\Sigma_{ij} = \alpha^{|i-j|}$ and α refers to the lag-1 AC value (Methods). The subscript r denotes rural. With this assumption, the estimation error for δHDP notably decreases (Fig. 3). For 2-day heat events, the RMSE is 0.019 in the GFDL model and 0.033 in the CLM model (Fig. 4a,b), and equation (3) can explain 87.4% of the diagnosed δHDP in the GFDL model and 92.2% in the CLM model (Fig. 3a,b). For 3-day heat events, the RMSE is 0.025 in the GFDL model and 0.038 in the CLM model (Fig. 4c,d), and equation (3) can explain 73.9% of the diagnosed δHDP in the GFDL model and 88.1% in the CLM model (Fig. 3c,d). These results confirm the importance of the influence of temperature persistence on δHDP predictions for multi-day heat events, consistent with findings from previous research[10].

Moreover, according to a recent study[11], temperature persistence can be substantially different between urban and rural environments. Although the lag-1 AC values of either urban or rural temperatures differ between the GFDL and CLM models, the spatial patterns of urban–rural differences in lag-1 AC remain broadly consistent (Supplementary Fig. 4e,f), ranging from −0.13 to 0.16 in the GFDL model and from −0.07 to 0.23 in the CLM model. Both models show larger urban–rural differences near the equator, moderate differences across Europe and Southeast Asia, and smaller or even negative differences in southeastern South America. Therefore, we further extend the framework to account for urban–rural differences in lag-1 AC as follows:

$$\delta\mathrm{HDP} = \phi_N(\Gamma, \alpha_\mathrm{r}) - \phi_N(\Gamma - \delta Z, \alpha_\mathrm{u}), \quad (4)$$

where the subscript u denotes urban. After considering the urban–rural difference in temperature persistence, the RMSE further decreases to 0.018 (0.023) in the GFDL model and 0.030 (0.033) in the CLM model, and equation (4) can explain 88.9% (76.8%) of the diagnosed δHDP in the GFDL model and 92.6% (89.5%) in the CLM model for 2-day (3-day) heat events (Fig. 3). When the urban–rural differences in lag-1 AC exceed 0.1, accounting for the urban–rural differences in temperature persistence (equation (4)) reduces the error of predicting δHDP by 27.8% (26.3%) in the GFDL model and 29.1% (32.5%) in the CLM model (compared with equation (3)) for 2-day (3-day) heat events (Fig. 4). As before, we use the 90th percentile as the heat event threshold, but the above conclusions remain unchanged when using the 95th percentile threshold (Supplementary Figs. 5 and 6). Overall, these results suggest that for most regions, knowing only δZ and rural AC is enough to predict multi-day δHDP. However, for grid cells with strong urban–rural differences in lag-1 AC (Supplementary Fig. 4), knowing the urban–rural difference in AC is also crucial for accurately predicting multi-day δHDP.

Discussion and concluding remarks

In this study, we quantify the role of temperature mean, variability and persistence in contributing to urban–rural differences in the probability of hot day and multi-day heat event occurrences. The increased likelihood of hot days in urban areas, relative to rural areas, is almost entirely predicted by the standardized mean UHI effects. Discovering the importance of standardization is one of the main novelties of this work, namely, cities with more pronounced mean UHI effects and smaller temperature variabilities are more susceptible to increased

https://doi.org/10.1038/s44284-025-00290-2

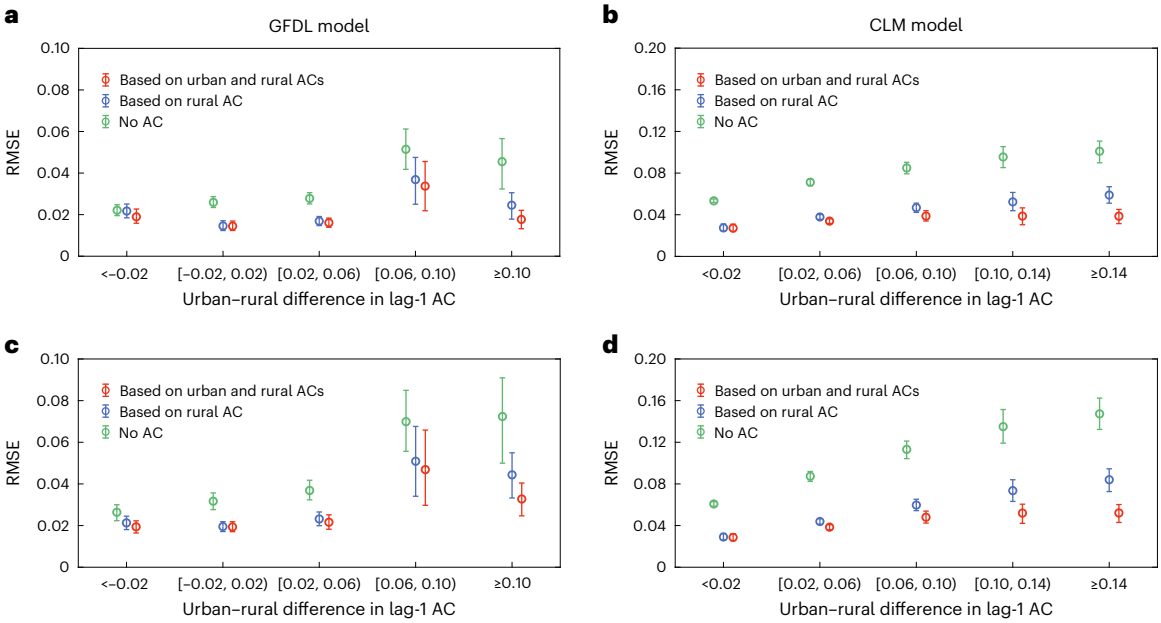

Fig. 4 | RMSE of predicted δHDP for multi-day heat events across different bins of urban–rural differences in lag-1 AC. a,**b**, Two-day heat events. **c**,**d**, Three-day heat events. Green bars illustrate δHDP predictions under the assumption that urban and rural daily mean temperatures are independent across days (equation (2)). Blue bars assume that urban and rural temperatures share the same lag-1 AC calculated from the rural temperature within each grid (equation (3)). Red bars use distinct lag-1 AC values for urban and rural temperatures calculated from their respective temperature series in each grid (equation (4)). The range of error bars indicates the 95% confidence intervals calculated using the non-parametric bootstrap percentile method, with 1,000 resamples across valid grid cells within each bin. Left column: results from the GFDL model (**a** and **c**); right column: from the CLM model (**b** and **d**).

hot day occurrence. This key finding explains why a previous study found stronger contrasts between urban and rural heat event trends in wet climates, which are associated with smaller variability in the UHI intensity[19]. Furthermore, our statistical model shows that the relationship between the mean urban warming and the likelihood of extreme urban temperatures is a nonlinear function of standardized mean UHI. The growth rate of urban–rural differences in the probability of hot day occurrence accelerates most rapidly when the standardized mean UHI is in the range of 0.5–2; under these conditions, implementing heat mitigation measures can yield the greatest benefits in reducing the likelihood of extreme urban temperatures.

For multi-day heat events, the standardized mean UHI remains important but the role of temperature persistence cannot be ignored, as assuming no AC in the temperature time series does not adequately capture urban–rural differences in the probability of multi-day heat event occurrence. In particular, accounting for urban–rural differences in temperature persistence can further help predict urban–rural differences in the probability of multi-day heat events regionally, especially in places where the urban temperature persistence is notably stronger than its rural counterpart. It is worth noting that although the two global models we use differ in mean UHI, temperature variability and persistence (possibly due to differences in atmospheric forcing data and other model input data, as well as model-specific physical parameterizations), our main finding that the standardized mean UHI and temperature persistence are sufficient for predicting the simulated urban–rural differences in heat event occurrence is consistent and robust across models.

A potential caveat of our study is the use of global climate models, which operate at relatively coarse spatial resolutions and force urban and rural areas within the same grid cell to be influenced by the same atmospheric condition, regardless of whether the land model is coupled to the atmosphere model[20,21]. This setup may dampen local feedbacks that influence urban temperature variability[22], but the magnitude of this effect is uncertain. Comparing variability in the observed temperature series would be a helpful check, but station-based temperature data come with their own uncertainties[23], especially due to breakpoints from location changes and urbanization. Correcting these issues, especially in daily data, remains challenging[24]. Hence, despite the large computations involved, using mesoscale modeling (for example, with the Weather Research and Forecasting model), where urban and rural areas each interact with the respective atmospheric conditions, would also be an alternative and crucial future undertaking.

Nevertheless, our result reveals the fundamental interaction between temperature mean, variance and persistence in shaping urban–rural difference in the probability of hot day and multi-day heat event occurrences and has crucial implications for future urban planning and heat management. Traditionally, urban heat mitigation efforts often focus on reducing the mean UHI. However, the differences in hot day occurrence between urban and rural areas are not solely determined by the mean UHI. Thus, depending on the baseline temperature variability, reducing the mean UHI by the same magnitude can yield different outcomes in terms of reducing urban hot day occurrences. For example, it would tend to be more effective over humid regions, which generally have smaller temperature variance, than arid and semiarid regions[19]. Moreover, accounting for temperature persistence is crucial for multi-day heat events. For example, cities clustered with metal roofs tend to have larger thermal inertia and, hence, greater temperature persistence compared with surrounding rural areas[11], which would further prolong heat events and exacerbate health impacts. As a result, cities with stronger mean UHI effects, smaller temperature variances and higher thermal inertia should prioritize mitigating the negative impacts of extreme heat.

Methods

Model simulations

The GFDL land model LM4 (ref. 25), coupled with a newly developed and evaluated UCM[26,27], and the CLM version 5 (ref. 28), which is the land component of the CESM version 2.0.1 (ref. 29), are used to simulate urban and rural temperatures in this study.

The LM4 is a comprehensive land surface model developed by the GFDL[25], which is part of the National Oceanic and Atmospheric Administration. This model is designed to simulate biophysical and biogeochemical processes to understand and predict how these processes affect the Earth's climate and how they are affected by the changing climate. Coupled with the UCM, the LM4 can solve the energy and water balances for urban and rural areas covered by different land cover types (that is, natural and secondary vegetation, pasture and grassland), respectively, within each grid cell. Comprehensive descriptions of the physical process parameterizations pertinent to urban environments, encompassing aspects of urban vegetation, are provided elsewhere[26,27]. These studies also documented evaluations of the UCM's effectiveness in capturing fluxes. In this study, the Sheffield forcing, which is generated based on observations and reanalysis data with a 1° spatial resolution and a three-hourly temporal resolution[30], is used to drive the LM4 coupled with the UCM. We conducted the simulations at 2 latitude × 2.5 longitude from 1700 to 2000, with the period of 1700–1948 for spin up, and focused on the simulations of the latest 40-year period from 1961 to 2000 for our analysis. An extensive appraisal of the modeled urban and rural temperature patterns is presented elsewhere[31].

The CLM is also an advanced land surface model, which is fully coupled with the CESM, and provides state-of-the-art simulations of the Earth's past, present and future climate states. Within each grid cell, multiple land units, including vegetated, lake, urban, glacier and crop, are designed to independently exchange energy, momentum and water with the atmosphere in the CLM. The processes over the urban land unit are parameterized by the urban surface scheme of the CLM, known as CLM Urban. This scheme conceptualizes urban areas as a two-dimensional canyon structure comprising five distinct facets: roof, sun-shaded wall, sun-lit wall, pervious ground and impervious ground. Further details regarding the CLM Urban parameterization is provided elsewhere[29,32]. Here we run the CLM (uncoupled to the atmospheric model) at 0.9 latitude × 1.25 longitude based on an initial condition provided by the CESM, which is spin up by the Global Soil Wetness Project Phase 3 atmospheric forcing from 1970 to 2010 (ref. 28). For the analysis, we focused on the simulations of the latest 40-year period from 1971 to 2010.

UHI calculation

Unlike mesoscale modeling or observational studies in which UHIs are typically calculated as the temperature difference between urban and its surrounding rural areas, this approach is not feasible at the global scale due to the coarse horizontal resolution of global climate simulations. Therefore, in this study, the UHI is defined as the surface air temperature difference between urban (simulated by the UCM) and non-urban land types within the same grid cell. Specifically, in the GFDL model, urban temperatures are derived from the urban tile, which includes both roof and canyon components. In the CLM model, urban temperatures are calculated by the CLM Urban for the urban land unit. Rural temperatures are computed using an area-weighted average of non-urban land cover types within each grid cell. This involves natural vegetation, secondary vegetation, pasture and grassland tiles in the GFDL model, and vegetated and crop land units in the CLM model.

It is important to note that in both models, the properties of urban land units are derived from a global dataset developed in ref. 33, and urban fractions are held constant throughout the simulation period (Supplementary Fig. 7). Furthermore, our analysis focus on grid cells in which the urban fraction exceeds 0.1%, as the model does not perform calculations for urban land units with a fractional coverage below this threshold[28].

Identifying heat events

In this study, heat events are identified based on daily mean surface air temperatures in summer (that is, June, July and August for the Northern Hemisphere, and December, January and February for the Southern Hemisphere) derived from the GFDL and CLM simulations. Before identifying heat events, we take specific steps to isolate the heat signal from the long-term trends and seasonal cycles. First, to eliminate long-term temperature trends due to global warming, we apply a linear detrending method to both urban and rural temperature time series. Specifically, for each grid cell, we fit a least squares linear regression line to the summer daily mean temperatures over the analysis period and subtract the fitted trend from the original time series to obtain the detrended temperature series. Second, to remove interseasonal signals, we calculate the multi-year daily climatology of rural temperatures by averaging rural daily mean temperatures for each calendar day in summer across all years. This assumes that rural areas are not subject to anthropogenic influences and, thus, provide a baseline for natural interseasonal variability. We then subtract this climatological seasonal cycle from both urban and rural detrended temperature series to obtain the anomaly series that exclude interseasonal variations. This process filters out the seasonal cycles of urban and rural temperatures and retains their respective long-term means.

After detrending and removing the interseasonal signals, we define heat events as periods of single hot days or as periods of at least two or more consecutive days in summer during which the daily mean temperature exceeds its 90th or 95th percentile from 1961 to 2000 in the GFDL simulations and from 1971 to 2010 in the CLM simulations. Specially, urban and rural hot day occurrences, denoted as HDP_u and HDP_r, respectively, are computed using the same temperature threshold defined based on rural temperature climatology.

Standardized Gaussian framework for understanding and predicting urban–rural differences in the probability of hot day and multi-day heat event occurrences

We assume that both urban and rural temperatures follow a Gaussian distribution:

$$f(x) = \frac{1}{\sigma\sqrt{2\pi}} e^{-\frac{1}{2}\left(\frac{x-\mu}{\sigma}\right)^2}, \tag{5}$$

where μ is the mean of the distribution, and σ is the standard deviation. The corresponding CDF can be expressed as

$$F(x) = \frac{1}{2}\left[1 + \mathrm{erf}\left(\frac{x-\mu}{\sigma\sqrt{2}}\right)\right]. \tag{6}$$

When heat events are defined as periods of single hot days, we can write

$$\mathrm{HDP_r} = 1 - P_\mathrm{T} = 1 - \frac{1}{2}\left[1 + \mathrm{erf}\left(\frac{T_\mathrm{r}^\mathrm{p} - \mu_\mathrm{r}}{\sigma_\mathrm{r}\sqrt{2}}\right)\right], \tag{7}$$

$$\mathrm{HDP_u} = 1 - \frac{1}{2}\left[1 + \mathrm{erf}\left(\frac{T_\mathrm{r}^\mathrm{p} - \mu_\mathrm{u}}{\sigma_\mathrm{u}\sqrt{2}}\right)\right], \tag{8}$$

where μ_u and μ_r are the mean of the urban and rural temperature, respectively, whereas σ_u and σ_r are the corresponding standard deviations. T_r^p is the threshold value calculated based on the rural temperature profile, utilized to delineate the threshold for heat events. P_T represents the percentile thresholds. For instance, for temperature thresholds of 90th or 95th percentile, the corresponding P_T values are 0.9 or 0.95, respectively.

According to equation (7), we can write

$$P_\mathrm{T} = \phi(\Gamma) = \frac{1}{2}\left[1 + \mathrm{erf}\left(\frac{\Gamma}{\sqrt{2}}\right)\right], \tag{9}$$

where

$$\Gamma = \frac{T_r^p - \mu_r}{\sigma_r}. \tag{10}$$

Hence, equation (8) can be simplified as

$$\begin{aligned} \mathrm{HDP_u} &= 1 - \tfrac{1}{2}\left[1 + \mathrm{erf}\left(\tfrac{T_r^p - \mu_u}{\sigma_u\sqrt{2}}\right)\right] = 1 - \tfrac{1}{2}\left[1 + \mathrm{erf}\left(\tfrac{\sigma_r}{\sigma_u}\tfrac{T_r^p - \mu_r}{\sigma_r\sqrt{2}} - \tfrac{\mu_u - \mu_r}{\sigma_r\sqrt{2}}\right)\right] \\ &\approx 1 - \tfrac{1}{2}\left[1 + \mathrm{erf}\left(\tfrac{T_r^p - \mu_r}{\sigma_r\sqrt{2}} - \tfrac{\mu_u - \mu_r}{\sigma_r\sqrt{2}}\right)\right] = 1 - \tfrac{1}{2}\left[1 + \mathrm{erf}\left(\tfrac{\Gamma}{\sqrt{2}} - \tfrac{\delta Z}{\sqrt{2}}\right)\right] \\ &= 1 - \phi(\Gamma - \delta Z) \end{aligned} \tag{11}$$

To derive the above equation, we have assumed $\sigma_u \approx \sigma_r$ and denote $\delta Z = \frac{\mu_u - \mu_r}{\sigma_u} \approx \frac{\mu_u - \mu_r}{\sigma_r}$. Therefore, the urban–rural difference in the probability of hot day occurrence can be expressed as

$$\begin{aligned} \delta\mathrm{HDP} &= \mathrm{HDP_u} - \mathrm{HDP_r} = [1 - \phi(\Gamma - \delta Z)] - [1 - \phi(\Gamma)] \\ &= \phi(\Gamma) - \phi(\Gamma - \delta Z). \end{aligned} \tag{12}$$

When heat events are defined as periods lasting at least two or more consecutive days, we design three different models using different assumptions related to temperature persistence. Our first model assumes that both urban and rural temperatures are independent across days. Therefore, urban–rural differences in the probability of N-day heat event occurrence (that is, urban–rural differences in the yearly sum of days participating in N-day heat events) can be simply expressed by an N-dimensional Gaussian distribution:

$$\delta\mathrm{HDP} = \phi_N(\Gamma) - \phi_N(\Gamma - \delta Z), \tag{13}$$

where ϕ_N is the CDF of an N-dimensional Gaussian distribution centered on zero, and the first input of ϕ_N is an $N \times 1$ vector, with each element being the same as $\Gamma - \delta Z$ or Γ.

Our second model assumes that urban and rural share a same lag-1 AC calculated from the rural temperature. Hence, the urban–rural difference in the probability of N-day heat event occurrence can be expressed as

$$\delta\mathrm{HDP} = \phi_N(\Gamma, \alpha_r) - \phi_N(\Gamma - \delta Z, \alpha_r), \tag{14}$$

where ϕ_N is the CDF of an N-dimensional multivariate Gaussian distribution centered on zero as before and with covariance matrix Σ defined as $\Sigma_{ij} = \alpha^{|i-j|}$. The subscript r denotes rural.

Our third model accounts for the urban–rural difference in temperature persistence as follows:

$$\delta\mathrm{HDP} = \phi_N(\Gamma, \alpha_r) - \phi_N(\Gamma - \delta Z, \alpha_u), \tag{15}$$

where the subscript u denotes urban.

Reporting summary

Further information on research design is available in the Nature Portfolio Reporting Summary linked to this article.

Data availability

Data generated in this study are available on Zenodo at https://doi.org/10.5281/zenodo.15131945 (ref. 34) and are publicly accessible.

Code availability

Analysis code used in this study is available on Zenodo at https://doi.org/10.5281/zenodo.15131945 (ref. 34). MATLAB R2022b is used to analyze the data.

References

1. Meehl, G. A. & Tebaldi, C. More intense, more frequent, and longer lasting heat waves in the 21st century. *Science* **305**, 994–997 (2004).
2. Frölicher, T. L., Fischer, E. M. & Gruber, N. Marine heatwaves under global warming. *Nature* **560**, 360–364 (2018).
3. Wang, J. et al. Anthropogenically-driven increases in the risks of summertime compound hot extremes. *Nat. Commun.* **11**, 528 (2020).
4. Pfleiderer, P., Schleussner, C.-F., Kornhuber, K. & Coumou, D. Summer weather becomes more persistent in a 2 °C world. *Nat. Clim. Change* **9**, 666–671 (2019).
5. Sun, Y. et al. Rapid increase in the risk of extreme summer heat in Eastern China. *Nat. Clim. Change* **4**, 1082–1085 (2014).
6. Li, J. & Thompson, D. W. J. Widespread changes in surface temperature persistence under climate change. *Nature* **599**, 425–430 (2021).
7. Simolo, C. & Corti, S. Quantifying the role of variability in future intensification of heat extremes. *Nat. Commun.* **13**, 7930 (2022).
8. Chan, D., Cobb, A., Zeppetello, L. R. V., Battisti, D. S. & Huybers, P. Summertime temperature variability increases with local warming in midlatitude regions. *Geophys. Res. Lett.* **47**, e2020GL087624 (2020).
9. Mearns, L. O., Katz, R. W. & Schneider, S. H. Extreme high-temperature events: changes in their probabilities with changes in mean temperature. *J. Appl. Meteorol. Climatol.* **23**, 1601–1613 (1984).
10. Barnston, A. G., Lyon, B., Coffel, E. D. & Horton, R. M. Daily autocorrelation and mean temperature/moisture rise as determining factors for future heat-wave patterns in the United States. *J. Appl. Meteorol. Climatol.* **59**, 1735–1754 (2020).
11. Li, D. et al. Persistent urban heat. *Sci. Adv.* **10**, eadj7398 (2024).
12. Kalnay, E. & Cai, M. Impact of urbanization and land-use change on climate. *Nature* **423**, 528–531 (2003).
13. Sun, Y., Zhang, X., Ren, G., Zwiers, F. W. & Hu, T. Contribution of urbanization to warming in China. *Nat. Clim. Change* **6**, 706–709 (2016).
14. Manoli, G. et al. Magnitude of urban heat islands largely explained by climate and population. *Nature* **573**, 55–60 (2019).
15. Zhao, L., Lee, X., Smith, R. B. & Oleson, K. Strong contributions of local background climate to urban heat islands. *Nature* **511**, 216–219 (2014).
16. Zhou, L. et al. Evidence for a significant urbanization effect on climate in China. *Proc. Natl. Acad. Sci. USA* **101**, 9540–9544 (2004).
17. Zhao, L. et al. Global multi-model projections of local urban climates. *Nat. Clim. Change* **11**, 152–157 (2021).
18. Domeisen, D. I. V. et al. Prediction and projection of heatwaves. *Nat. Rev. Earth Environ.* **4**, 36–50 (2023).
19. Liao, W. et al. Stronger contributions of urbanization to heat wave trends in wet climates. *Geophys. Res. Lett.* **45**, 1131–1140 (2018).
20. Oleson, K. W., Bonan, G. B. & Feddema, J. Effects of white roofs on urban temperature in a global climate model. *Geophys. Res. Lett.* **37**, L03701 (2010).
21. Wang, L., Huang, M. & Li, D. Where are white roofs more effective in cooling the surface? *Geophys. Res. Lett.* **47**, e2020GL087853 (2020).
22. Seneviratne, S. I. et al. Investigating soil moisture–climate interactions in a changing climate: a review. *Earth Sci. Rev.* **99**, 125–161 (2010).
23. Trewin, B. Exposure, instrumentation, and observing practice effects on land temperature measurements. *WIREs Climate Change* **1**, 490–506 (2010).
24. Chan, D., Gebbie, G. & Huybers, P. An improved ensemble of land surface air temperatures since 1880 using revised pair-wise homogenization algorithms accounting for autocorrelation. *J. Clim.* **37**, 2325–2345 (2024).

25. Zhao, M. et al. The GFDL global atmosphere and land model AM4.0/LM4.0: 2. Model description, sensitivity studies, and tuning strategies. *J. Adv. Model. Earth Syst.* **10**, 735–769 (2018).
26. Li, D., Malyshev, S. & Shevliakova, E. Exploring historical and future urban climate in the Earth System Modeling framework: 1. Model development and evaluation. *J. Adv. Model. Earth Syst.* **8**, 917–935 (2016).
27. Li, D., Malyshev, S. & Shevliakova, E. Exploring historical and future urban climate in the Earth System Modeling framework: 2. Impact of urban land use over the Continental United States. *J. Adv. Model. Earth Syst.* **8**, 936–953 (2016).
28. Lawrence, D. M. et al. The Community Land Model version 5: description of new features, benchmarking, and impact of forcing uncertainty. *J. Adv. Model. Earth Syst.* **11**, 4245–4287 (2019).
29. Danabasoglu, G. et al. The Community Earth System Model version 2 (CESM2). *J. Adv. Model. Earth Syst.* **12**, e2019MS001916 (2020).
30. Sheffield, J., Goteti, G. & Wood, E. F. Development of a 50-year high-resolution global dataset of meteorological forcings for land surface modeling. *J. Clim.* **19**, 3088–3111 (2006).
31. Liao, W. et al. Amplified increases of compound hot extremes over urban land in China. *Geophys. Res. Lett.* **48**, e2020GL091252 (2021).
32. Oleson, K. W. & Feddema, J. Parameterization and surface data improvements and new capabilities for the Community Land Model Urban (CLMU). *J. Adv. Model. Earth Syst.* **12**, e2018MS001586 (2020).
33. Jackson, T. L., Feddema, J. J., Oleson, K. W., Bonan, G. B. & Bauer, J. T. Parameterization of urban characteristics for global climate modeling. *Ann. Assoc. Am. Geogr.* **100**, 848–865 (2010).
34. Liao, W., Wang, L., Liu, X., Chan, D. & Li, D. Standardized heat islands and persistence drive modelled urban heat events—supporting data. *Zenodo* https://doi.org/10.5281/zenodo.15131945 (2025).

Acknowledgements

X.L. acknowledges support from the National Science Fund for Distinguished Young Scholars (grant no. 42225107). W.L. acknowledges support from the National Natural Science Foundation of China (grant no. 42271419), Innovation Group Project of Southern Marine Science and Engineering Guangdong Laboratory (Zhuhai) (grant no. 311021004), and Fundamental Research Funds for the Central Universities, Sun Yat-sen University (grant no. 23lgbj014). D.L. acknowledges support from the US Department of Energy, Office of Science, as part of research in MultiSector Dynamics, Earth and Environmental System Modeling Program.

Author contributions

W.L. designed the study, carried out the analysis and wrote the paper. L.W. performed the simulations. X.L. designed and supervised the study. D.C. and D.L. designed the study and wrote the paper.

Competing interests

The authors declare no competing interests.

Additional information

Supplementary information The online version contains supplementary material available at https://doi.org/10.1038/s44284-025-00290-2.

Correspondence and requests for materials should be addressed to Xiaoping Liu, Duo Chan or Dan Li.

Peer review information *Nature Cities* thanks Matteo Zampieri and the other, anonymous, reviewer(s) for their contribution to the peer review of this work.